

Measuring cluster temperatures via kinetic-energy release

Peter Brockhaus,¹ Kin Wong,¹ Klavs Hansen,² Vitaly Kasperovich,¹ George Tikhonov,¹ and Vitaly V. Kresin¹

¹*Department of Physics and Astronomy, University of Southern California, Los Angeles, California 90089-0484*

²*Institute of Physics and Astronomy, University of Aarhus, Ny Munkegade, Bygn. 520, DK-8000 Aarhus C, Denmark*

(Received 22 June 1998)

We use photodissociation of neutral sodium clusters to measure the recoil pattern of the fragmentation products. The time dependence of the depletion curves reflects the kinetic-energy release that depends on the internal energy, or the temperature, of the cluster. The fragmentation process is treated parallel to the Weisskopf statistical theory of the disintegration of compound nuclei. From the kinetic energies of evaporation, we are able to determine the temperatures of both the daughter and mother clusters. For Na₂₀ the temperature is found to be $T=440\pm 65$ K, which is in good agreement with an estimate based on the evaporative ensemble model. The measured temperature is slightly larger than that found for large ionic clusters. Branching ratios for the evaporation of sodium dimers and monomers from hot neutral clusters are estimated. [S1050-2947(99)01301-3]

PACS number(s): 36.40.Qv, 82.20.Db, 82.50.Fv

I. INTRODUCTION

The study of free metal nanoclusters in beams is a powerful technique, giving one the ability to perform spectroscopy on particles of a precisely determined size and undisturbed by the presence of a matrix. There is, however, an important characteristic which has been rather difficult to establish for a beam of isolated clusters: their temperature distribution. The internal vibrational temperature of metallic clusters influences not only their optical properties [1,2], but also their chemical properties [3,4], heat capacity [5], ionization thresholds [3,6–9], and even the mass abundance spectra [10,11].

The search for a “cluster beam thermometer” is non-trivial, because the conventional technique of vibrational spectroscopy can be applied only to very small species, e.g., alkali dimers [12,13]. However, the temperatures of larger clusters are known to be dramatically different [14]. Other techniques, such as rotational spectroscopy [12,15], are not sufficiently accurate because the rotational temperature of clusters is typically not in equilibrium with the vibrational temperature.

A significant insight into the thermal state of free clusters in a beam was provided by Gspann [16]. In this picture (later termed “evaporative ensemble” by Klots [17,18]), cluster sources produce particles in a state of high thermal excitation. Freshly formed clusters evaporate atoms or fragments as they leave the hot nozzle of a typical source. The size distribution observed at the detector therefore reflects the result of at least one such evaporative process per arriving cluster.

This is a valuable picture, because it permits one to estimate the temperature of clusters arriving at the detector based on their dissociation energies D and flight times. The typical time it takes a particle of N atoms, originally at temperature T , to evaporate an atom is given by

$$\tau \approx \frac{\tau_0}{N^{2/3}} e^{D/k_B T}. \quad (1)$$

Here the $N^{2/3}$ factor corresponds to the cluster surface area, and τ_0 is a characteristic time factor (see Sec. III). The particles arriving at the detector are already sufficiently cold to not have evaporated any more atoms during their flight time from the source (otherwise they would have been removed from the beam by the resulting recoil, see below). Therefore, the evaporation lifetimes of these clusters must be at least an order of magnitude longer than the typical flight time, i.e., $\geq 10^{-2}$ s. One can now approximately relate the vibrational temperatures of the arriving clusters to their atomic binding energies,

$$k_B T \approx D/G, \quad (2)$$

where $G \approx \ln(\pi/\tau_0)$ is the so-called Gspann parameter. Its magnitude is clearly not very sensitive to the precise values of the relevant lifetimes, and is typically given as $G \sim 25-30$.

This picture is applicable to nanoclusters which fragment by successive evaporation events, and provides a first approximation to the energetics of hot, free clusters. For example, it has been used to establish a rigorous connection between the abundance spectra of large sodium clusters and their intrinsic electronic shell structure [11,19,20]. In this way, an estimate for the effective overall temperature can be obtained; however, the temperatures of the individual cluster sizes can differ noticeably, especially for the smaller clusters [14].

More detailed studies of metal cluster evaporation have employed photodissociation of cluster ions. By preselecting a particular size in a mass spectrometer, one can focus on the fragmentation kinetics of a specific cluster. It has been found that the absorption of a photon by the cluster electrons (e.g., via the giant collective dipole resonance [21]) is very rapidly followed by thermalization into the vibrational degrees of freedom and subsequent evaporation of atoms or dimers. This forms the basis of cluster-beam depletion spectroscopy [22]. The thermally excited intermediate state of the cluster is analogous to the compound nucleus picture well known in

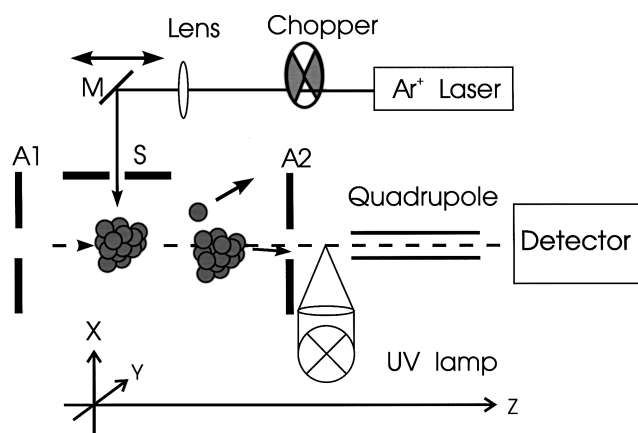


FIG. 1. Outline of the experimental principle. Absorption of a photon sets off a chain of evaporation events. Recoil following fragmentation reduces the probability of the daughter cluster entering the detection region. By measuring the decay of the daughter cluster signal as the distance between the laser spot and the detector aperture increases, we can determine the daughter and mother cluster temperatures.

nuclear physics. The statistical Weisskopf treatment of compound nuclei [23,24], based on detailed-balance considerations, relates the rate constants of the evaporation channels and the fragment energy distribution to the daughter nucleus temperature.

This formalism can be carried over to cluster and molecular fragmentation as well. It shares a common basis with RRK and RRKM statistical theories of unimolecular dissociation [25–27]. These models have been used to fit the dissociation rates of photoexcited metal cluster ions [28–30], and to derive an estimate of the cluster temperatures and binding energies for charged sodium clusters [14]. In a kinematic experiment [31], Hansen and Falk measured the momentum distribution of atoms evaporating from large sodium cluster ions (Na_N^+ , $N \sim 10^3$) to unambiguously assign the average parent ion-beam temperature.

The aforementioned experiments have all been conducted on cluster ions. However, there is an extensive amount of spectroscopic data available for small and medium-sized neutral clusters, and it is of significant interest to gain temperature information about these species. This is nontrivial, however, because in general one can neither size select a particular precursor from a beam of neutrals nor mass analyze the photodissociation products.

In this paper, we describe a determination of the temperature of the neutral Na_{20} cluster formed in a supersonic expansion source by a technique which measures its recoil following an evaporation event. The clusters are illuminated by a laser beam a certain distance away from the detector entrance aperture. By varying this distance and measuring the parent and daughter intensity changes, we can quantify the fragmentation pathways as well as recover the daughter and parent temperatures.

We chose Na_{20} as the model system for several reasons. First of all, it is a prototypical closed-shell cluster, and as such has been widely studied, but a number of unresolved questions remain. In particular, they concern the effect of vibrational excitations on the cluster response properties. For example, it is recognized that the vibrational temperature has

a strong influence on the shape and width of dipole resonance absorption [1]; it also appears to affect the static polarizability [32]. Second, it represents one of the dominant magic numbers in the sodium cluster mass spectrum, and its abundance compared to the larger neighbors (see Fig. 2) ensures a strong fragmentation signal without significant contamination from other cluster sizes.

In Sec. II, we describe the experimental principle and setup. Section III outlines the analysis of the data and the temperature fitting procedure. The results are presented in Sec. IV, and in Sec. V they are discussed and compared with other measurements.

II. EXPERIMENT

The experimental setup is schematically shown in Fig. 1. The supersonic expansion source used here is identical to the one described in Refs. [33,34]. A steel oven filled with sodium is maintained at 595°C . The sodium vapor is forced through a nozzle ($T = 770^\circ\text{C}$) by argon as a carrier gas at a pressure of 700 kPa, and subsequently passes a skimmer. The speed of the clusters has been measured to be 1100 ± 30 m/s (for Na_{20}) [34]. The beam travels freely for a distance of 2.0 m until it reaches a circular aperture (A1) with a diameter of 3.175 mm. This aperture serves to define the size of the photofragmenting beam. Immediately after the aperture, the cluster beam is illuminated perpendicularly by a chopped 3-W multimode argon-ion laser. The strongest lines are 514.5 and 488 nm, which add up to approximately 80% of the total laser output power. Wavelengths below 435 nm are cut off with a filter (Schott GG435). This gives us an average photon energy of 2.5 eV. The laser beam is pre-expanded by a cylindrical lens and passes through a 1 mm wide slit (S), so that the cluster beam is illuminated uniformly across by a narrow band of light with a fluence of 0.9 W/mm^2 . This gives a cluster signal depletion of up to 30%.

A second circular detector aperture (A2) with a diameter of 1.27 mm is located behind the laser-cluster interaction region. The principle of the experiment can be seen from the figure: photodissociation of the mother cluster results in the recoil of the daughter cluster; however, if the daughter is born sufficiently close to the detector aperture it will still pass through the latter and be registered. The probability of this occurring depends on the distance to the aperture and on the kinetic energy release during evaporation (and thereby on the cluster temperature).

The distance between the laser spot and the aperture can be varied between 10 and 42 mm. The clusters which pass through the aperture are ionized by a filtered (Schott UG 11) Hg-Xe UV lamp. The filter is chosen to provide photons at an energy close to the ionization threshold to minimize ionization-induced fragmentation [34–36]. The light from the UV lamp is focused to a spot size of 3 mm. The ionized clusters are subsequently mass selected by a quadrupole mass spectrometer and detected using a Daly dynode detector [37].

The data is collected by a personal computer which also controls the mass filter. The depleted and undepleted signals were detected quasisimultaneously by chopping the argon-ion laser at a frequency of 150 Hz. In a typical run, the mass

range Na_{16} to Na_{20} is divided into channels, each with a pair of bins. The mass spectrometer is set to a specific channel and after each laser pulse the bins record both the “laser-on” and “laser-off” counts. After ten laser pulses the mass spectrometer advances to the next channel, until the entire mass range is covered. In Ref. [38] this mode is referred to as a “gated mass scan.” For each laser-detector distance, 100 passes through the chosen mass range are averaged. The complete measurements are repeated several times, and found to give consistent results. The data presented below represent the average of several experimental runs.

Following a photoabsorption event, the intensity of a particular cluster signal, e.g., Na_{18} (see Fig. 4) changes due to two different reactions. One is the fragmentation of Na_{18} into smaller clusters, with a probability α . This depletion is not dependent upon the laser-detector distance L . The second one is the fragmentation of Na_{20} into Na_{18} , a process which is assigned a weight R^{-1} . This contribution increases as the distance L decreases. Since we are interested in the channel where the mother cluster Na_{20} fragments into the daughter cluster Na_{18} , we normalize the measured Na_{18} signal as follows:

$$S_{18}(L) = R \frac{\text{Na}_{18}(\text{laser on}) - \text{Na}_{18}(\text{laser off}) \times \alpha}{\text{Na}_{20}(\text{laser off}) - \text{Na}_{20}(\text{laser on})}. \quad (3)$$

Both constants R and α are determined directly from the signal. The former is used to normalize the data. The latter is found as follows. For large distances L the Na_{18} signal which originated from Na_{20} is proportional to the solid angle spanned by the detector aperture, as seen from the mother cluster at the point where it fragments. In other words, the Na_{18} daughter cluster signal is proportional to $1/L^2$ for large L . Therefore, α is obtained by plotting $\text{Na}_{18}(\text{laser on})/\text{Na}_{18}(\text{laser off})$ versus $1/L^2$, and extrapolating a straight line to $L = \infty$.

The fraction of the mother clusters Na_{20} which fragments must appear in the daughter cluster mass channels. The Na_{20} signal itself is not affected by fragmentation of larger clusters because the amount of Na_{21} , Na_{22} , and Na_{23} clusters are 10% or less of the amount of Na_{20} clusters; see Fig. 2. This is confirmed by the observation that the $\text{Na}_{20}(\text{laser on})$ signal does not vary with L .

The steepness and curvature of the $S_N(L)$ depletion curves obtained as shown in Eq.(3) depends on the recoil of the daughter cluster Na_N and therefore on its temperature. In Sec. III we describe how these curves are fitted to an evaporation model.

III. ANALYSIS OF EVAPORATION KINETICS

The clusters heated by the laser cool by evaporating either monomers (Na) or dimers (Na_2). Since the process is assumed to be statistical in nature, and the clusters have many internal vibrational degrees of freedom, it can be appropriately described by the Weisskopf theory [23,24] originally developed to describe disintegration of the compound nucleus state. This formalism predicts the following probability distribution for the relative kinetic energy ϵ of the fragments:

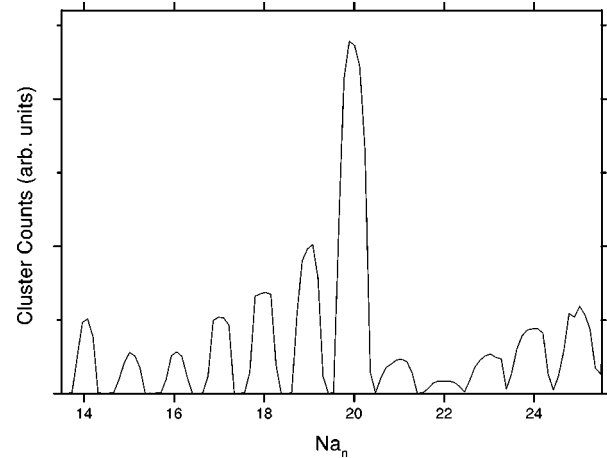


FIG. 2. A typical mass spectrum for the range Na_{14} to Na_{25} .

$$I(\epsilon)d\epsilon = A \epsilon e^{-\epsilon/k_B T} d\epsilon. \quad (4)$$

As noted in Sec. I, this equation is derived from general considerations based on detailed-balance requirements. The factor of ϵ arises as a measure of the phase space available for translational motion, and the Arrhenius exponential factor describes the final internal density of states of the daughter cluster. It is important to point out that the temperature appearing in Eq. (4) is that of the daughter cluster. For an individual particle with total internal energy E_0 and many excited internal degrees of freedom, the rigorous definition of the temperature is [23,24]

$$\frac{1}{T_0} = k_B \left. \frac{\partial(\ln W)}{\partial E} \right|_{E=E_0}, \quad (5)$$

where W is the level density of internal states accessible at this excitation energy. The prefactor A in Eq. (4) is proportional to the cross section for the reverse process, i.e., for the capture of an atom by a neutral cluster. In our calculation it is taken to be independent of ϵ , which is equivalent to the assumption of a constant sticking coefficient and no activation barrier. This is expected to be a good approximation for thermal neutral atom-cluster collisions. Indeed, the fits described below support the lack of any strong energy dependence of A . As discussed in Sec. V, the situation in experiments involving cluster ions appears to be different.

Armed with a predicted kinetic-energy distribution, we simulated the evaporation process using a Monte Carlo approach. We assume that all mother clusters enter the first aperture ($A1$ in Fig. 1) moving at the same speed parallel to the beam axis (z direction) and are equally distributed over the plane of the aperture. This is justified by the large distance to the source (2 m) and the small opening of the molecular-beam aperture (3.175 mm). The simulation of a fragmentation process starts with a cluster assigned to a random point in the laser-cluster beam interaction plane. The recoil of the daughter cluster from the fragmentation process is calculated (the direction of the departing fragment is also taken to be random). If more than one evaporation process occurs, appropriate energy distributions are calculated for each consecutive evaporation step. The directions of fragment emissions are assumed to be uncorrelated. This leads to

a velocity in the x and y directions, as well as to a small correction to the initial velocity in the z direction. The cluster is then propagated from the interaction region to the detector aperture (A2 in Fig. 1). In the plane of the detector aperture, the position of the daughter cluster is evaluated. If it can enter the detector, it is counted as a hit.

A typical simulation involves 100 000 such processes. After the complete simulation, the number of hits is divided by the number of clusters in the simulation, and normalized to the ratio of the areas of the apertures A1 and A2. For the next step in the simulation, the distance between laser interaction region and detector aperture is varied. The curves are fit to the data by minimizing χ^2 with the temperature as fit parameter.

Once the temperature of the daughter cluster is obtained, the temperature of the mother cluster can also be derived if its dissociation energy is known. Since there is no experimental data for neutral clusters available, we use the values for dissociation energies of ionic clusters as derived by Bréchnignac *et al.* [14] from the unimolecular photofragmentation patterns using a model given by Engelking [27]. The data from the cluster with the same number of valence electrons are taken; e.g., if we want to know the dissociation energy of the reaction $\text{Na}_{18} \rightarrow \text{Na}_{17} + \text{Na}$, we use the value given for Na_{19}^+ . We refrained from using a Born-Haber cycle to derive the dissociation energies for neutrals. The uncertainties in the available data for ionization potentials are fairly large, and the measurements are not always consistent. For example, Refs. [6] and [9,39] give values that differ by as much as 0.3 eV depending on the cluster size.

Based on the values of the dissociation energies as given by Ref. [14], and on the mother cluster temperatures extracted from the experimental data (see below), the characteristic fragmentation time τ_0 used in the evaporation rate equation (1) is required to be on the order of 10^{-12} s for monomer evaporation, which is equivalent to a Gspann parameter of 25. Lower values would yield unrealistic lifetimes for the clusters arriving from the source. Other estimates of τ_0 are available in the literature [40–43], but they would imply a change in the dissociation energies by $\sim 10\%$ [44]. For consistency, we shall adhere to the aforementioned values of D and τ_0 . The possible error introduced by the use of these values is taken into account in the overall experimental uncertainty.

The reduction in the number of degrees of freedom following the evaporation has to be taken into account. For the case of monomer evaporation, this gives

$$(3N-6)k_B T_{\text{mother}} = \{[3(N-1)-6]+2\}k_B T_{\text{daughter}} + D. \quad (6)$$

We have made the usual assumption of equipartition between all the vibrational degrees of freedom in the cluster. This assumption in fact coincides with what one obtains by applying the definition of temperature [Eq. (5)] to the density of states of an ensemble of coupled classical oscillators (the Kassel model [25,26,45,46]). The change in the electronic degrees of freedom and free energy is contained within the separation energies D [47]. The extra term of $2k_B T_{\text{daughter}}$ on the right-hand side accounts for the average kinetic energy of the evaporating particle [24].

For dimers, the connection is slightly more complicated, because the dimer has two rotational degrees of freedom, with energy $k_B T/2$ each, and one vibrational degree of freedom with $k_B T$. Making the assumption that the temperature of the dimer is the same as of the daughter cluster, we have

$$(3N-6)k_B T_{\text{mother}} = \{[3(N-2)-6]+4\}k_B T_{\text{daughter}} + D. \quad (7)$$

To calculate the temperature of the mother cluster before heating with the argon-ion laser, the following formula is applied:

$$(3N-6)k_B T_{\text{before}} + h\nu = (3N-6)k_B T_{\text{after}}. \quad (8)$$

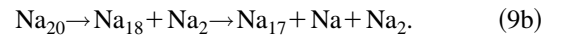
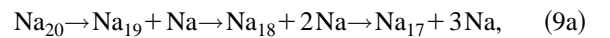
Thus we can obtain the original temperature of the mother cluster in the beam.

IV. RESULTS

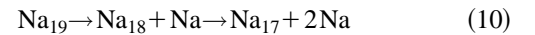
The experimental results obtained for Na_{17} are depicted in Fig. 3; for Na_{16} and Na_{18} , see Fig. 4. These graphs also show the results of our Monte Carlo simulations.

Since the decay of the measured signal is a function of the recoil of the daughter clusters due to the evaporation of small fragments, we have to look into the possible fragmentation pathways. This will first be done for the Na_{17} cluster because it gives by far the largest signal.

Possible reaction pathways leading to this cluster mass from the mass with the largest abundance, Na_{20} , are either the evaporation of monomers as described by Eq. (9a) or of a dimer and a monomer (9b). We do not include the evaporation of a dimer from an odd-electron system, as it has never been experimentally observed [14]:



Further contributions could stem from the fragmentation of Na_{19} as given by Eq. (10). But this gives only a small correction, since the abundance of Na_{20} is nearly four times larger than that of Na_{19} (see Fig. 2). This is also included in our fit:



These are the only significant sources of detectable Na_{17} products. Indeed, those that derive from the photofragmentation of Na_{18} are so hot that, according to Eq. (1) (see also Ref. [41]), they will decay further before they arrive at the detector [cf. Eq. (A2e)]. The evaporation chains for all clusters larger than Na_{20} , on the other hand, will effectively terminate before reaching this mass.

The possible pathways are used to perform fits to fragment temperatures according to the Weisskopf formalism as described in Sec. III. Two different temperature schemes are obtained: Pathway (9a) gives consecutive temperatures for the fragments of $T(\text{Na}_{19}) = 865$ K, $T(\text{Na}_{18}) = 685$ K, and $T(\text{Na}_{17}) = 480$ K. This yields a temperature for the mother cluster Na_{20} of 515 K before its interaction with the laser. The second possibility [Eq. (9b)] gives temperatures of

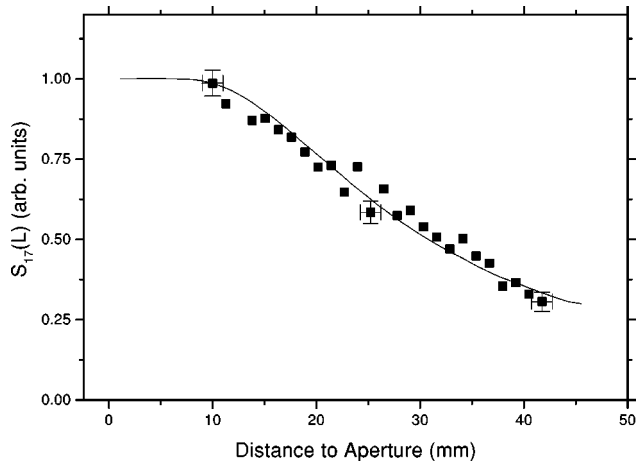


FIG. 3. Squares: Measured intensity of the Na_{17} signal as a function of the laser-detector distance. Solid line: Fit to the data for $T(\text{Na}_{20}) = 440$ K and evaporation channels (9b) and (10).

$T(\text{Na}_{18}) = 780$ K and $T(\text{Na}_{17}) = 575$ K, respectively. The temperature of the mother cluster $T(\text{Na}_{20})$ is 440 K in this case.

The decision which of these two pathways is the most important can be made using the data for Na_{18} . Since this is a somewhat elaborate procedure, it will be discussed in the Appendix, where the fits to the data for Na_{16} and Na_{18} are derived. We conclude that pathway (9a) makes only a minor contribution, and the data are mostly governed by the dissociation channel (9b). The initial temperature of the Na_{20} cluster is therefore determined to be 440 K. We also establish that for the Na_{18} cluster, the signal observed is mostly due to fragmentation of Na_{20} and Na_{21} while for Na_{16} the mother clusters are Na_{20} and Na_{18} .

Since we have considered all possible fragmentation pathways, we can estimate the relative contributions from dimer and monomer evaporation. There is a strong difference between the photodissociation pathways of Na_{20} and Na_{18} . In the former case the evaporation of a dimer is four times more likely than of a monomer. The ratio is nearly reversed in the case of Na_{18} , where the evaporation of a monomer is more probable by a factor of 3.

We have performed an extensive error analysis using Monte Carlo simulations to estimate the total uncertainty in the temperature of the Na_{20} cluster. We included experimental errors, (e.g., misalignment, fluctuations of the laser or the source, and the cluster speed distribution) as well as possible errors in the fitting procedure (the branching ratios for the different reactions, the derivation of α , uncertainties in the photon energy and in the dissociation energies for the different fragmentation pathways). From a statistical analysis of our data, we estimate our overall error to be ± 65 K.

Two possible additional sources of systematic error should be mentioned. The first one is post-ionization fragmentation. As mentioned in Sec. II, this effect is expected to be small in the present setup thanks to the use of soft near-threshold ionization.

The second effect is the presence of slow decay components in the ensemble of evaporating clusters, stemming from the fact that there is a certain initial temperature spread among the mother clusters. According to the evaporative en-

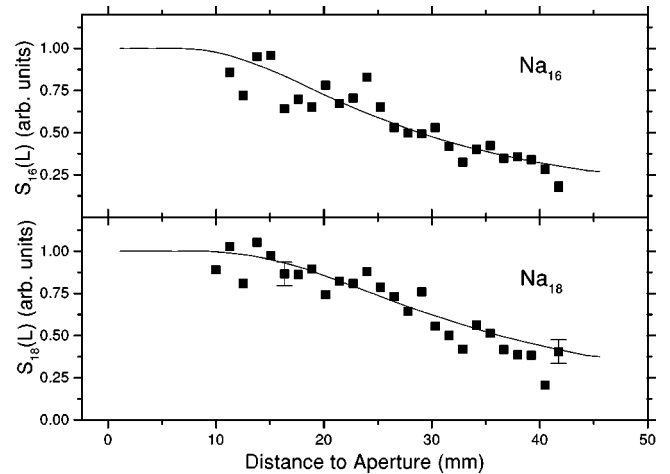


FIG. 4. Squares: Measured intensities of the Na_{16} (top) or Na_{18} (bottom) signals. Solid line: Fit to the data for $T(\text{Na}_{20}) = 440$ K and evaporation channels (A2a) and (A2e) for Na_{16} and (A1b) and (A1c) for Na_{18} .

semble formalism, the internal energy distribution of clusters in the beam has a full width approximately equal to the cluster dissociation energy [11,18–20]. With a Na_{20} binding energy of approximately 0.93 eV [14], this corresponds to a temperature spread of $\Delta T \approx \pm 100$ K. To assess the effect of this distribution, we performed a further Monte Carlo simulation which included the contribution of delayed fragmentation of the colder clusters. We found that with the average mother cluster temperature of 440 K, as determined above, and a ± 100 -K spread, we retain a good fit to the experimental profiles. On the other hand, increasing ΔT further would lead to a noticeable deviation of the simulated signal curves from the data. Our results are therefore quite consistent with the prediction of evaporative ensemble theory.

V. DISCUSSION AND SUMMARY

We have described an approach for measuring the internal temperature of free neutral metal clusters in a beam. Absorption of a photon by a cluster sets off a fragmentation chain whereby the cluster successively evaporates atoms and dimers as it cools down in the process. Kinetic energy released upon evaporation is found by studying the recoil of the daughter fragment. By employing the Weisskopf statistical theory, we can model the decay process and determine both the fragment temperatures and, as a consequence, the temperature of the original mother cluster.

This method was applied to Na_{20} clusters, photodissociated by 2.5-eV photons. The most important final products of the evaporation chains are Na_{18} , Na_{17} , and Na_{16} . The Na_{17} fragment, which gave the strongest signal, arises primarily via the decay chain [Eq. (9b)]. The experiment is assisted by the fact that Na_{20} is a dominant magic number in the mass spectrum, ensuring that contamination of the signal by fragmentation of larger species is negligible.

The average temperature of Na_{20} originally present in the beam is found to be 440 ± 65 K. By comparison, the source nozzle temperature was approximately 1040 K.

We can compare the temperature measured here with other experiments and expectations in several ways. One is a

direct comparison with the temperature distributions in Ref. [14], which result as a product of fitting dissociation energies of positively charged clusters. The distribution for Na_{21}^+ was estimated to range from ca. 250 to 580 K, corresponding to an average value of 415 K, as compared to the value of 440 K measured here (with an estimated range of ± 100 K).

A more precise comparison should take into account two effects. One is the difference in the charge state of the clusters involved, and the other is the flight time of the cluster beams, which was ~ 1 ms in the present case and ~ 10 μs in the experiment of Br chignac *et al.* The temperature of an evaporative ensemble decreases with time, and although this change is slow [logarithmic; cf. Eq. (2)], here it would amount to about 20%. This implies that on the time scale of our experiment, the centroid of the fitted ionic temperature distribution [14] would shift to 330 K, a value somewhat lower than the present measurement, but not outside the limits of experimental uncertainties.

Alternatively, one can compare the measured temperature to the one expected from evaporative ensemble theory [18]. A more accurate version of the estimate given in Eq. (2) reads as follows:

$$k_B T = D/G - k_B \Delta T + D/[2(3N - 6)], \quad (11)$$

where the second term on the right-hand side corrects for the fact that the original Gspann relation actually corresponds to the upper edge of the temperature distribution, and the third term is a correction for the finite heat capacity of the cluster [18]. Using $\Delta T \approx 100$ K and $D = 0.93$ eV for monomer evaporation, and the corresponding value of $G \approx 25$ (as described in Sec. III), we obtain $T = 410$ K, i.e., a value very close to the measured one. The close agreement between experiment and prediction affirms the validity of the evaporative ensemble picture.

An analysis of rate equations for the evaporative cooling of neutral Na_n ($n = 200 - 5000$) clusters using bulk liquid sodium parameters [45] also predicts a temperature of ~ 400 K at the end of a 2-ms flight time. The cooling rates turn out to be quite similar for different cluster sizes.

The experiments by Hansen and Falk [31] on large Na_n^+ ions ($n \sim 10^3$) gave a value of either 270 or 350 K (± 100 K), depending on the assumed capture cross section prefactor A in the evaporation energy distribution [Eq. (4)]. These values are slightly lower than our results, but note that the cluster sizes and evaporation time scales are different. Our present data could be successfully explained without invoking an energy dependence of the sticking coefficient. Clearly, the atom-cluster potentials and the cross sections for attachment are quite different in the cases of charged and uncharged clusters. A complete description of this reverse process is an important experimental and theoretical challenge in cluster physics [48]. As in the work [31], no indication of a significant activation barrier (of magnitude $k_B T$ or higher) was found in our data.

Our study implies that in a cluster photofragmentation experiment it is crucial to ensure sufficient time and distance between the laser-cluster interaction and detection steps. For a finite beam diameter, the ‘‘contamination’’ by evaporation fragments decays slower than one might expect from simple geometrical considerations [38]. In particular, one has to be

careful when performing measurements on relatively weak cluster signals which are close to clusters with large abundances in the mass spectra, for example Na_{16} . By extrapolating our data to longer distances between the interaction zone and the detector, we conclude that a $\sim 5\%$ contribution from the fragmentation of larger cluster sizes can still be detected even if the time delay between laser illumination and detection is as long as 100 μs .

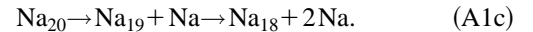
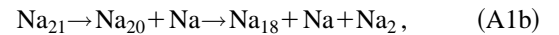
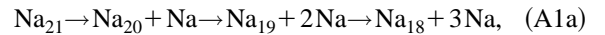
ACKNOWLEDGMENTS

We would like to thank W. Knight and A. Hirt for helpful discussions, and the staff of the Natural Sciences Machine Shop for expert technical help. This work was supported by the National Science Foundation under Grant No. PHY-9600039 and by the Danish National Research Foundation through the research center ACAP with a grant to K.H.

APPENDIX A: FRAGMENTATION PATHWAYS

1. Simulation of the Na_{18} signal

In order to decide which of pathways (9a) or (9b) is the strongest, we have to look at the data for the Na_{18} cluster. This signal could stem from the fragmentation of Na_{21} or Na_{20} as described by Eqs. (A1a)–(A1c):



We do not need to include single-evaporation pathways directly from Na_{20} or from Na_{19} , e.g., $\text{Na}_{19} \rightarrow \text{Na}_{18} + \text{Na}$, because these would create the Na_{18} cluster in too hot a state to survive until the detection (cf. the discussion of Na_{17} in Sec. IV).

Channels (A1a) and (A1b), while possibly present, cannot be a strong source of Na_{18} products: the abundance of Na_{21} clusters is only 10% of Na_{20} , and the signal they can contribute would be several times smaller than that observed (the ratio between the Na_{17} and Na_{18} fragment intensities is 5:1).

Thus the dominant Na_{18} signal must come from channel (A1c). Now, as described in Sec. IV, the two possible pathways (9a) and (9b) for the appearance of Na_{17} fragments imply two different initial temperatures for the Na_{20} mother cluster. An analysis of the Na_{18} signal can resolve the issue. Indeed, if we assume fragmentation pathway (9a) and start with a temperature of $T = 515$ K for Na_{20} before laser heating, this leads to a fragment temperature $T(\text{Na}_{18}) = 685$ K. However, this is inconsistent with the observations, because a fragment at this high a temperature will have an estimated lifetime [Eq. (1)] of only a few μs . Since the flight time from the interaction region to the detector is at least 10 μs , this cluster would never be detected in our setup. This makes the dissociation pathway (9a) unlikely.

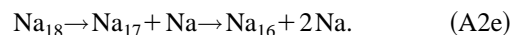
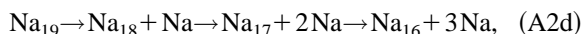
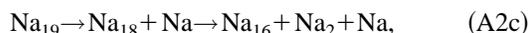
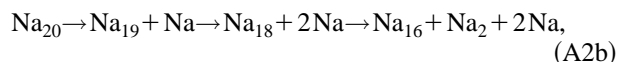
This leaves us with the pathway as described by Eq. (9b), where we obtained a temperature of the mother fragment Na_{20} of 440 K. Using dissociation pathway (A1c), we now determine a temperature of 600 K for the Na_{18} cluster. This

is still relatively hot, and will in principle lead to further fragmentation. But the lifetime here is dramatically longer than in the preceding scenario (using the Gspann formalism, we obtain a factor of 10).

Indeed, if we assume a lifetime of $\geq 200 \mu\text{s}$, we obtain an even better fit to our data than what is given in Fig. 4. Further fragmentation would lead to Na_{17} via monomer evaporation: $\text{Na}_{18} \rightarrow \text{Na}_{17} + \text{Na}$. The complete reaction pathway would be the same as Eq. (9a), but with a lower starting temperature for the mother cluster Na_{20} . The contribution from this reaction to the Na_{17} mass channel is small, because otherwise the Na_{17} signal would be strongly distorted due to lifetime effects. By simulating a continuous evaporation scheme, as indicated here, we estimate this contribution to the Na_{17} signal to be below 10%. In summary, we conclude pathway (9b) to be the most favorable, and will in the further discussion neglect fragmentation channel (9a).

2. Simulation of the Na_{16} signal

Analogously to Na_{18} , it is possible to derive a fit to the data for the Na_{16} cluster. But in this case several other fragmentation channels play a role due to the larger abundance of Na_{19} and Na_{18} , namely,



Pathway (A2a) only differs from Eq. (9b) by the evaporation of a dimer from Na_{18} instead of a monomer. Since the signal on the Na_{17} mass channel is at least five times larger than on the Na_{16} channel, we conclude that monomer evaporation is in this case much more likely than dimer evaporation. For the same reason we can neglect pathway (A2c): the abundance of the mother cluster Na_{19} is lower than that of Na_{20} , and the last evaporation step is suppressed.

Reaction (A2d) seems unlikely, because it gives a larger temperature for Na_{19} than for Na_{20} . This is in contradiction to the assumption of an evaporative ensemble, which assumes that of two clusters with the same time for evaporation, the cluster with the lower binding energy will be colder.

We can now differentiate between pathway (A2b) on the one hand and pathways (A2a) and (A2e) on the other. For the former, we obtain a lower temperature for the daughter cluster than for the mother cluster, although the time for the mother cluster to cool down before it is again heated up by the laser is at least 50 times longer than the time for the daughter cluster to reach its final state. In principle, this is possible since the binding energies of these clusters are different.

We obtained the fit shown in Fig. 4 using only pathways (A2a) and (A2e), where we assumed that the temperature of Na_{18} as mother cluster is the same as that of Na_{20} . The quality of the fit does not improve by taking Eqs. (A2b) into account. We conclude that pathways (A2a) and (A2e) play the most important role, although further work is needed to clarify the various possibilities. The branching ratio between monomer and dimer evaporation from Na_{18} , used for the fit to the Na_{16} data, is 1:3.

-
- [1] C. Ellert, M. Schmidt, C. Schmitt, T. Reiners, and H. Haberland, *Phys. Rev. Lett.* **75**, 1731 (1995).
- [2] W. Saunders and N. Dam, in *Nuclear Physics Concepts in the Study of Atomic Cluster Physics*, edited by R. Schmidt, H. O. Lutz, and R. Dreizler (Springer, Heidelberg, 1992), Chap. 2, p. 93.
- [3] E. Honea, M. Homer, J. L. Persson, and R. Whetten, *Chem. Phys. Lett.* **171**, 147 (1990).
- [4] M. F. Jarrold, *J. Phys. Chem.* **99**, 11 (1995).
- [5] M. Schmidt, R. Kusche, B. von Issendorff, and H. Haberland, *Nature (London)* **393**, 238 (1998).
- [6] M. M. Kappes, M. Schär, U. Röthlisberger, C. Yeretizian, and E. Schuhmacher, *Chem. Phys. Lett.* **143**, 251 (1988).
- [7] W. A. Saunders, K. Clemenger, W. de Heer, and W. Knight, *Phys. Rev. B* **32**, 1366 (1985).
- [8] W. Saunders, Ph.D. thesis, University of California, Berkeley, 1986.
- [9] M. Homer, J. L. Persson, E. Honea, and R. Whetten, *Z. Phys. D* **22**, 441 (1991).
- [10] F. Chandezon, P. M. Hansen, C. Ristoni, J. Pedersen, J. Westergaard, and S. Bjørnholm, *Chem. Phys. Lett.* **277**, 450 (1997).
- [11] F. Chandezon, S. Bjørnholm, J. Borggreen, and K. Hansen, *Phys. Rev. B* **55**, 5485 (1997).
- [12] C. P. Schulz, R. Haugstätter, H. U. Tittes, and I. V. Hertel, *Phys. Rev. Lett.* **57**, 1703 (1986).
- [13] M. M. Kappes and S. Leutwyler, in *Atomic and Molecular Beam Methods*, edited by G. Scoles (Oxford, New York, 1988).
- [14] C. Bréchnignac, Ph. Cahuzac, J. Leygnier, and J. Weiner, *J. Chem. Phys.* **90**, 1492 (1988).
- [15] I. V. Hertel, C. P. Schulz, A. Goerke, H. Palm, and G. Leipelt, *J. Chem. Phys.* **107**, 3528 (1997).
- [16] J. Gspann, in *Physics of Electronic and Atomic Collisions*, edited by S. Datz (North-Holland, Amsterdam, 1986), pp. 79–96.
- [17] C. E. Klots, *J. Chem. Phys.* **83**, 5854 (1985).
- [18] C. E. Klots, *J. Phys. Chem.* **92**, 5864 (1988).
- [19] S. Bjørnholm, J. Borggreen, H. Busch, and F. Chandezon, in *Large Clusters of Atoms and Molecules*, edited by T. P. Martin (Kluwer, Dordrecht, 1996).
- [20] K. Hansen, *Surf. Rev. Lett.* **3**, 597 (1996).
- [21] V. V. Kresin, *Phys. Rep.* **220**, 1 (1992).
- [22] W. A. de Heer, *Rev. Mod. Phys.* **65**, 611 (1993).
- [23] J. M. Blatt and V. F. Weisskopf, *Theoretical Nuclear Physics* (Springer, Heidelberg, 1979).
- [24] T. Ericson, *Adv. Phys.* **9**, 425 (1960).
- [25] O. Rice and H. Ramsperger, *J. Am. Chem. Soc.* **49**, 1617 (1927).

- [26] P. J. Robinson and K. A. Holbrook, *Unimolecular Reactions* (Wiley, London, 1972).
- [27] P. C. Engelking, *J. Chem. Phys.* **87**, 936 (1987).
- [28] C. Bréchnignac, Ph. Cahuzac, F. Carlier, M. de Frutos, J. Leygnier, J. Ph. Roux, and A. Sarfati, *Comments At. Mol. Phys.* **31**, 361 (1995).
- [29] M. Jarrold, U. Ray, J. Bower, and K. Creegan, *J. Chem. Soc., Faraday Trans.* **86**, 2537 (1990).
- [30] U. Hild, G. Dietrich, S. Krückeberg, M. Lindinger, K. Lützenkirchen, L. Schweikhard, C. Walther, and J. Ziegler, *Phys. Rev. A* **57**, 2786 (1998).
- [31] K. Hansen and J. Falk, *Z. Phys. D* **34**, 251 (1995).
- [32] K. Clemenger, Ph.D. thesis, University of California, Berkeley, 1985.
- [33] W. de Heer, W. Knight, M. Y. Chou, and M. L. Cohen, in *Solid State Physics*, edited by H. Ehrenreich and D. Turnbull (Academic, New York, 1987), Vol. 40.
- [34] V. V. Kresin, V. Kasperovich, G. Tikhonov, and K. Wong, *Phys. Rev. A* **57**, 383 (1998).
- [35] U. Buck and H. Meyer, *Phys. Rev. Lett.* **52**, 109 (1984).
- [36] L. Bewig, U. Buck, C. Mehlmann, and M. Winter, *J. Chem. Phys.* **100**, 2765 (1993).
- [37] R. N. Daly, *Rev. Sci. Instrum.* **31**, 264 (1960).
- [38] K. Selby, M. Vollmer, J. Masui, V. Kresin, W. A. de Heer, and W. D. Knight, *Phys. Rev. B* **40**, 5417 (1989).
- [39] J. L. Persson, Ph.D. thesis, University of California, Los Angeles, 1991.
- [40] G. F. Bertsch, N. Oberhofer, and S. Stringari, *Z. Phys. D* **20**, 123 (1991).
- [41] U. Näher and K. Hansen, *J. Chem. Phys.* **101**, 5367 (1994).
- [42] S. Frauendorf, *Z. Phys. D* **35**, 191 (1995).
- [43] P. Fröbrich, *Phys. Lett. A* **202**, 99 (1995).
- [44] P. Brockhaus, K. Wong, and V. V. Kresin (unpublished).
- [45] P. Fröbrich, *Ann. Phys. (Leipzig)* **6**, 403 (1997).
- [46] Although the heat capacity of a molten cluster is larger than that of a system of simple harmonic oscillators [5], it has been shown by Fröbrich [45] that calculations using the entropy of bulk liquid sodium predict cluster cooling rates quite close to those of the oscillator model.
- [47] K. Hansen and M. Manninen, *J. Chem. Phys.* **101**, 10481 (1994).
- [48] R. Schmidt and H. O. Lutz, *Comments At. Mol. Phys.* **31**, 461 (1995).